



Growth and atomic structure of tellurium thin films grown on Bi_2Te_3

Yuma Okuyama^a, Yuya Sugiyama^a, Shin-ichiro Ideta^b, Kiyohisa Tanaka^b,
Toru Hirahara^{a,*}

^a Department of Physics, Tokyo Institute of Technology, Tokyo 152-8551, Japan

^b UVSOR Facility, Institute for Molecular Science, Okazaki 444-8585, Japan



ARTICLE INFO

Article history:

Received 16 October 2016

Received in revised form

21 November 2016

Accepted 24 November 2016

Available online 29 November 2016

Keywords:

Tellurium

Thin film

Epitaxial growth

Strain

ABSTRACT

We have grown tellurium (Te) thin films on Bi_2Te_3 and investigated the atomic structure. From low-energy electron diffraction (LEED) measurements, we found that the Te films are [1010]-oriented with six domains. A detailed analysis of the reflection high-energy electron diffraction (RHEED) pattern revealed that the films are strained with the in-plane lattice constant compressed by ~1.5% compared to the bulk value due to the epitaxy between Te and Bi_2Te_3 . These films will be interesting systems to investigate the predicted topological phases that occur in strained Te.

© 2016 Elsevier B.V. All rights reserved.

1. Introduction

Chirality is a geometric property of materials and is mostly discussed in chemistry or biology [1]. A chiral molecule/ion is non-superposable on its mirror image (enantiomers) and individual enantiomers are often called as either “right-” or “left-handed”. Some solid crystals also have chirality such as elements tellurium (Te) and selenium (Se). As shown in Fig. 1(a), they are trigonal structures that can be regarded as a hexagonal array of helical chains at ambient pressure. They lack inversion symmetry and possess chirality depending on the rotation direction of the screw axis. Namely, right- and left-handed chirality correspond to the structures shown in Fig. 1(b) and (c). Due to this peculiar crystal structure, Te shows intriguing properties such as the circular photon drag effect [2] or the current-induced spin polarization [3,4].

It is also well known that the physical properties of Te and Se can be tuned by controlling the lattice constant, which can be achieved by applying pressure [5,6]. They will eventually undergo a structural transition to the monoclinic or the triclinic phases at very high pressure in the order of ~10 GPa. The electronic structure can also be changed from a semiconductor (the band gap is 0.33 eV and 2.0 eV for Te and Se, respectively) to a metal by applying pressure. Recently, based on *ab initio* calculations, it was predicted that

Te undergoes a trivial insulator to a strong topological insulator (metal) transition under shear (hydrostatic or uniaxial) strain in the trigonal phase [7]. Furthermore, it was predicted that the lack of inversion symmetry and spin-orbit interaction leads to the existence of Dirac points or Weyl nodes in the band structure of Te or Se [8]. Such states possess an unconventional spin texture and furthermore, if one can fine-tune the lattice constant by carefully controlling the applied pressure, Te and Se are expected to show the Weyl semimetal phase [9].

An alternative way to change the lattice constant of a material is to grow thin films and utilize the epitaxy with the substrate. Such method has been applied to Bi films grown on Bi_2Te_3 and showed a change in their topological properties [10]. Thin film growth of Te has actually been performed from the monolayer regime [11] to relatively thick films [12,13]. The main purpose to grow thick Te films was to use them as capping layers to protect the topological surface states in air. Thus, it did not matter whether the grown Te was amorphous or granular, but it turned out that the grown Te films were crystalline. Tellurium films grown on Bi_2Te_3 showed clear low-energy electron diffraction (LEED) and reflection high-energy electron diffraction (RHEED) patterns [12], and X-ray diffraction measurements showed that Te films grown on Cr-doped $(\text{Bi},\text{Sb})_2\text{Te}_3$ (CBST) are oriented in the [1010] direction [13].

In the present study, we performed a detailed investigation of the atomic structure of Te films grown on Bi_2Te_3 to see if these films are strained or not. To the best of our knowledge, such experimental effort has not been performed previously. From RHEED and LEED

* Corresponding author.

E-mail address: hirahara@phys.titech.ac.jp (T. Hirahara).

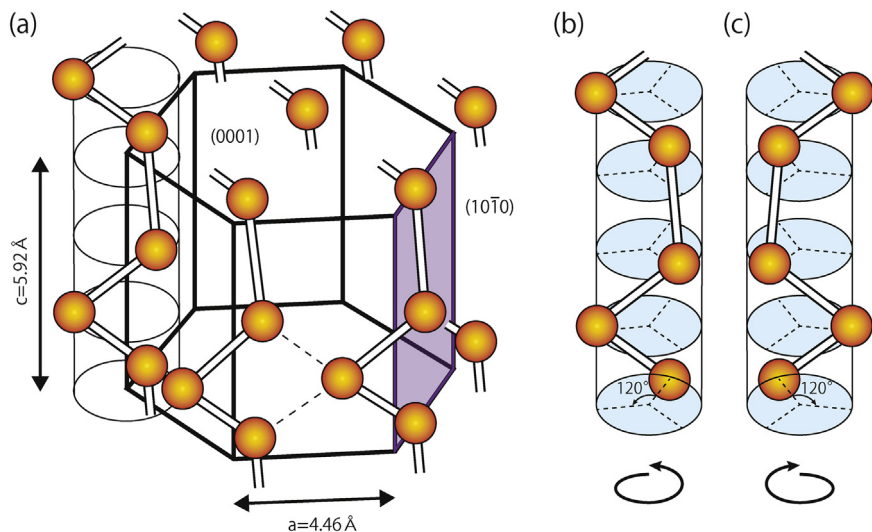


Fig. 1. (a) Schematic drawing of the chiral crystal structure of Te and Se. Right- and left-handed chiral structures are shown in (b) and (c), respectively.

measurements, we found that the grown Te films are six-domain ($[10\bar{1}0]$) films and the lattice constant is compressed by $\sim 1.5\%$ compared to the bulk values due to the epitaxial growth and the slightly different lattice constants between Te and Bi_2Te_3 . Thus, they should be an interesting system to study the possible realization of topological phases in Te.

2. Experimental

The experiments were conducted in ultrahigh vacuum chambers and RHEED was used to monitor the sample growth. Molecular beam epitaxy was employed as the deposition method. The fabrication of the substrate Bi_2Te_3 was the same as that reported previously. First, a clean Si(111)- 7×7 surface ($3 \text{ mm} \times 15 \text{ mm} \times 0.5 \text{ mm}$) was prepared on an n-type substrate (P-doped, $1\text{--}10 \Omega \text{ cm}$ at room temperature) by a cycle of resistive heat treatments. Then Bi was deposited on the 7×7 surface at 200°C in a Te-rich condition. This results in a quintuple-layer-by-quintuple-layer [(QL), $1 \text{ QL} = 10.2 \text{ \AA}$] $\text{Bi}_2\text{Te}_3(111)$ epitaxial film formation with bulk-like crystal structure [10,14,15]. The thickness of the Bi_2Te_3 films used in the present study was $\sim 15 \text{ QL}$. Tellurium was deposited on Bi_2Te_3 at room temperature. The deposition rate of Te was calibrated by the time it took to cover the Si(111)- 7×7 surface and was determined as 0.2 ML/min ($1 \text{ ML} = 3.8 \times 10^{14} \text{ atoms/cm}^2$, the atomic density of the Te($[10\bar{1}0]$) surface). Judging from the atomic structure of bulk Te shown in Fig. 1, we believe that Te grows in a trilayer-by-trilayer mode for the $[10\bar{1}0]$ orientation and one trilayer (3 ML) corresponds to a thickness of $\sim 3.9 \text{ \AA}$. LEED observations were performed after the sample fabrication at room temperature.

3. Results and discussion

Figure 2(a) shows the RHEED pattern of a 15 QL thick $\text{Bi}_2\text{Te}_3(111)$ film grown on Si(111). The incident energy of the electron beam was 15 keV. The 1×1 periodicity can be observed clearly showing both the zeroth and first Laue zones. Note that due to the limited domain size of the films, the spots are elongated in the vertical direction and look more like streaks. This kind of streak feature is quite often found in RHEED patterns of thin films, in contrast to the sharp RHEED spots of semiconductor clean surfaces such as Si(111)- 7×7 . Fig. 2(b), (c), and (d) show the RHEED patterns after 12 ML (16 Å) (b), 36 ML (47 Å) (c), and 60 ML (78 Å) (d) of Te deposition on the Bi_2Te_3 substrate at room temperature, respectively. One can see that the streaks of the first Laue zone

of Bi_2Te_3 have disappeared completely and more streaks can be found around the zeroth Laue zone. There are no significant differences between Fig. 2(b)–(d) although slight changes in the spot intensity can be found. So we think that the structure of the Te film does not change for different film thickness. In fact, the RHEED patterns for the film thinner than 12 ML showed a pattern that can be interpreted as an overlap of the streaks of Bi_2Te_3 and Te. Thus we suspect that the Te film has the same structure already from the initial stage of film growth. This is in sharp contrast to other cases such as Bi films grown on Si(111)- 7×7 , where an allotropic transformation has been confirmed [17]. The overall features shown in Fig. 2(b)–(d) are similar to that reported in Ref. [12].

Since it seemed difficult to determine the surface periodicity from the complicated RHEED patterns shown in Fig. 2(b)–(d), we performed LEED observation of the grown Te films. Fig. 3(a) shows the LEED pattern of the 60 ML Te film grown on Bi_2Te_3 . The incident energy was 21.5 eV. Although the background level is quite high, one can notice spot structures which are similar to that reported in Ref. [12]. In Ref. [12], no detailed structure determination based on LEED was performed and the complicated pattern was just interpreted as a result of the multidomain growth mode. Fig. 3(b) shows the spot positions of the LEED pattern in Fig. 3(a) for clarity. We first tried to assign a reciprocal lattice assuming only one domain, but it was not successful. We thus assumed a six-domain structure of a rectangular lattice. The different colors and symbols in Fig. 3(b) correspond to the different domains and the reciprocal unit cell for one of the domains is also indicated in Fig. 3(b). As shown in Fig. 3(c), one can explain almost all the observed spots assuming this structure (the open circles are the observed ones and the filled circles are the ones expected from the structure assumed). However, we found that the positions for the spots located at the periphery of the LEED screen showed a large deviation from their expected position. We think this is due to the flat MCP screen used in the LEED observation which can have a large influence on the spots far from the center, while those near the center are not much affected. Therefore, we believe that our structural analysis is correct and Te likely grows in a rectangular lattice. Roughly judging from the ratio of the long and short sides of the rectangle in Fig. 3, the film orientation is $[10\bar{1}0]$ (or any other equivalent direction).

In order to confirm our anticipation, we have analyzed the RHEED patterns of the Te films. We have found that when we assume that the electron beam is incident from the direction shown in Fig. 3(b), all the streaks in the RHEED pattern can be explained nicely as shown in Fig. 4(a). (As mentioned before, note that the

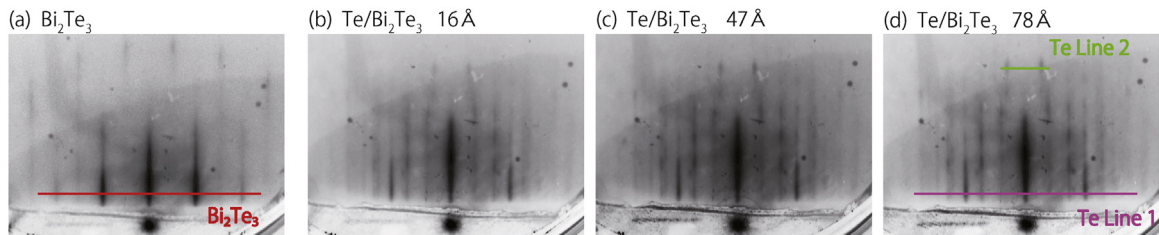


Fig. 2. RHEED patterns of the substrate Bi₂Te₃ (a), 16 Å thick Te film (b), 47 Å thick Te film (c), and 78 Å thick Te film (d), grown on Bi₂Te₃, respectively.

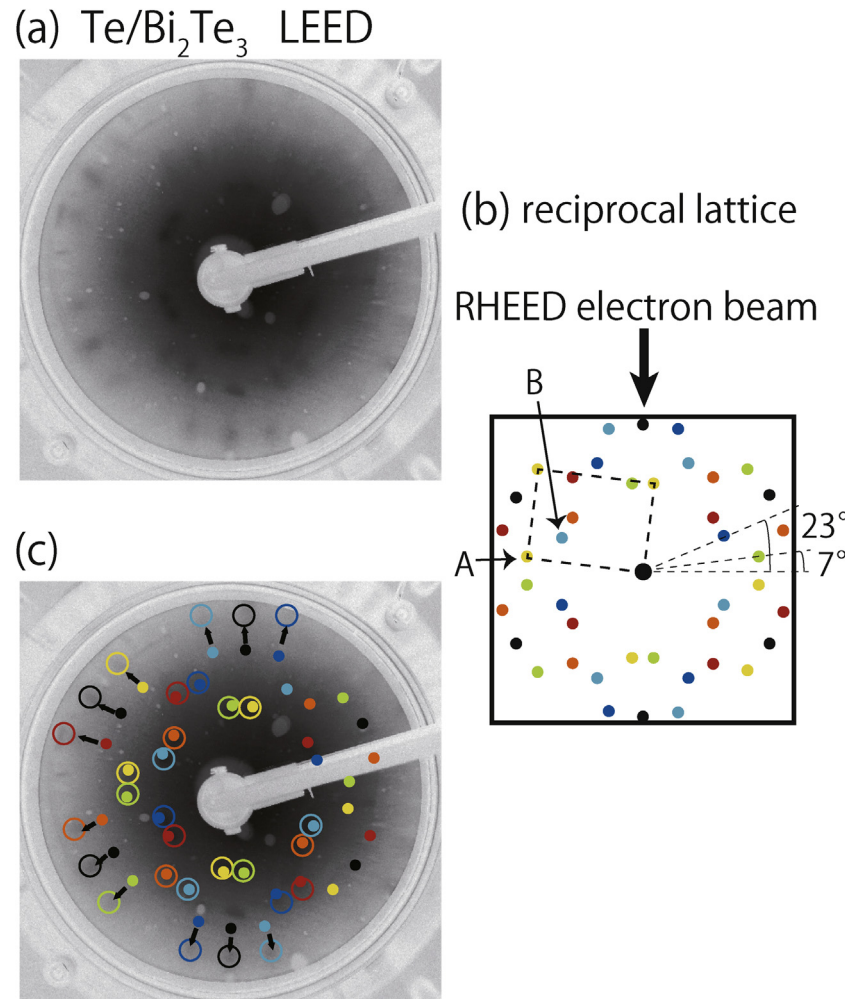


Fig. 3. (a) LEED pattern of the 78 Å thick Te film grown on Bi₂Te₃. (b) The reciprocal lattice derived from the LEED pattern in (a). The electron incident direction of the RHEED patterns is also indicated. Different colors represent different domains and the rectangular reciprocal unit cell for one of the domains is explicitly shown. A and B correspond to the spots in the RHEED pattern of Fig. 4(b). The angles between different domains are also shown. (c) Same as (a) but with the reciprocal lattice overlapped for clarity. (For interpretation of the references to color in this figure legend, the reader is referred to the web version of the article.)

vertical position is not so important due to the elongation of the spots.) A and B in Figs. 3(b) and 4(b) correspond to each other. Since we know the electron incident direction of the RHEED patterns with respect to the Bi₂Te₃(111) surface, we can determine the in-plane stacking direction between the multidomain Te(10̄10) and Bi₂Te₃(111). Furthermore, by comparing the streak spacing between the Bi₂Te₃ substrate and the grown Te films, the lattice constant of Te can be determined. Fig. 4(b) shows the line profiles of the RHEED streaks derived from the patterns in Fig. 2(a) and (d). For a quantitative analysis, first, a peak fit was performed to deduce the length of the arrow shown in Fig. 4(b) for Bi₂Te₃ (topmost arrow). This corresponds to $4\pi/a_{\text{Bi}_2\text{Te}_3}$. Then a peak fit

for the line profile of Te line 2 was performed and the arrow length was determined, which corresponds to $(4\pi/a)\cos 23^\circ$ (a is the short side of the rectangular unit cell). By taking the ratio of the length of the two arrows and using the lattice constant of Bi₂Te₃ ($a_{\text{Bi}_2\text{Te}_3} = 4.38 \text{ \AA}$), one obtains $a = 4.39 \pm 0.025 \text{ \AA}$. Similarly, a peak fit for the line profile of Te line 1 was performed and the length of the top arrow was deduced, which corresponds to $(4\pi/c)\cos 7^\circ$ (c is the long side of the rectangular unit cell). This results in $c = 5.85 \pm 0.052 \text{ \AA}$. The length of the remaining arrows in Fig. 4(b) was determined and we cross checked if the above analyses were reasonable using reciprocal spots from all the domains. As a result, we determined the in-plane lattice constants of the Te(10̄10) as

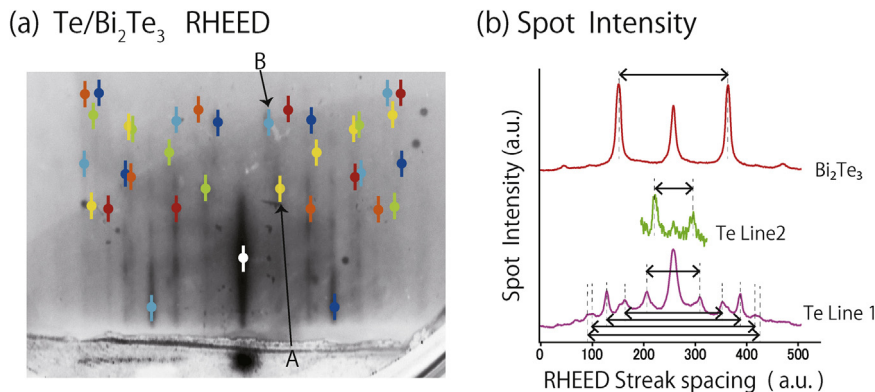


Fig. 4. (a) RHEED pattern of the 78 Å thick Te film grown on Bi_2Te_3 with the reciprocal lattice overlapped. Different colors represent different domains. A and B correspond to the reciprocal lattice shown in Fig. 3(b). (b) The RHEED spot intensity profile for the lines shown in Fig. 2. The distance of the indicated arrows was used in the quantitative analysis to deduce the real-space lattice constants (see the main text for details). (For interpretation of the references to color in this figure legend, the reader is referred to the web version of the article.)

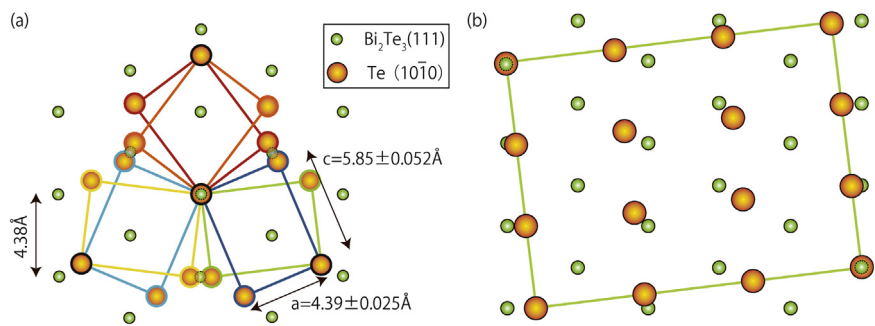


Fig. 5. (a) The real space lattice of the grown $\text{Te}(10\bar{1}0)$ films together with that of substrate Bi_2Te_3 . The lattice constants are shown explicitly. (b) The magic matching condition between Te and Bi_2Te_3 lattices ($5a_{\text{Bi}_2\text{Te}_3} \sim 3\sqrt{a^2 + c^2}$).

$a = 4.39 \pm 0.025 \text{ \AA}$ and $c = 5.85 \pm 0.052 \text{ \AA}$, respectively. Compared to the bulk values $a = 4.46 \text{ \AA}$ and $c = 5.92 \text{ \AA}$, they are compressed by 1.6% and 1.2%.

Figure 5(a) summarizes the structure in real space we have determined from LEED and RHEED concerning the $\text{Te}(10\bar{1}0)$ film grown on $\text{Bi}_2\text{Te}_3(111)$. A six-domain rectangular Te lattice grows on the single-domain hexagonal Bi_2Te_3 lattice. One can notice that the nearest-neighbor position is quite similar between the two with only $\sim \pm 7^\circ$ rotation. Compared to the $\text{Te}(10\bar{1}0)$ film grown on CBST, the Te domains of our films are rotated by 30° [13]. Since the lattice constant of CBST is $a_{\text{CBST}} = 4.28 \text{ \AA}$, which is only 0.1 \AA (2.3%) different with Bi_2Te_3 , it is quite interesting that such a small can induce a large difference in the in-plane orientation. In Ref. [13], it was shown that there is a lattice matching condition of $\sqrt{3}a_{\text{CBST}} \sim \sqrt{a^2 + c^2}$ between CBST and $\text{Te}(10\bar{1}0)$. In the present case of $\text{Te}/\text{Bi}_2\text{Te}_3$, we found a matching condition of $5a_{\text{Bi}_2\text{Te}_3} \sim 3\sqrt{a^2 + c^2}$ as shown in Fig. 5(b). Such commensurate relation is similar to that reported for $\text{Bi}(110)$ film growth on $\text{Si}(111)\sqrt{3} \times \sqrt{3}\text{-B}$ [16]. It would be interesting to tune the lattice constant of the substrate precisely and see how the Te film orientation, as well as the lattice constants, changes according to it.

Another interesting point that should be mentioned is that the lattice constant of the present Te films is different from the bulk value even for a relatively large film thickness (60 ML = 78 Å) and compressed by $\sim 1.5\%$. Intuitively, the lattice constant of a thin film should relax to its bulk value even when the first several layers grow epitaxially with the substrate. However, there are some cases where the matching condition makes the film strained even for relatively thick films such as Bi films grown on $\text{Si}(111)\sqrt{3} \times \sqrt{3}$ (the experimentally determined in-plane lattice constant was 4.48 Å, which was 1.3% smaller than the bulk value and this was

interpreted as due to the “magic mismatch” between Bi and the 7×7 surface) [17]. We believe that the matching condition of $5a_{\text{Bi}_2\text{Te}_3} \sim 3\sqrt{a^2 + c^2}$ is also quite dominant in determining the lattice constant in the present case. It has been shown that when a hydrostatic pressure is applied to Te, a decreases while c increases slightly [5]. Therefore we can also say that our films are strained in a unique manner that is not possible by just applying pressure, again suggesting the strong role of the substrate. Thus theoretical calculations for Te slabs strained in this intriguing way will be helpful in identifying the realization of topological phases in these films as well as experimental verification of the band structure. Furthermore, these films should possess chirality as shown in Fig. 1 and experimentally determining such property will be an important task as well as finding a way to grow the desired chirality.

4. Conclusions

In conclusion, we have fabricated Te thin films on Bi_2Te_3 . Through LEED and RHEED observations, we have determined that they are six-domain $[10\bar{1}0]$ -oriented films with the lattice constant contracted by $\sim 1.5\%$ compared to the bulk value due to the epitaxial relation of $5a_{\text{Bi}_2\text{Te}_3} \sim 3\sqrt{a^2 + c^2}$. These films should be intriguing in terms of verifying the predicted topological phases in strained Te. It would also be interesting to identify and control the chirality of the films and investigate how they affect the physical properties.

Acknowledgements

We acknowledge discussions with Motoaki Hirayama and Shuichi Murakami. This work has been supported by Grants-In-Aid from Japan Society for the Promotion of Science (Nos. 15H05453

and 16K13683) and the Toray Science Foundation. The LEED experiments were performed under the UVSOR Proposal Nos. 27-533, 28-526, and S-15-MS-0034.

References

- [1] J. Smith, *Organic Chemistry*, 4th ed., McGraw-Hill Education, 2013.
- [2] V.A. Shalygin, M.D. Moldavskaya, S.N. Danilov, I.I. Farbshtein, L.E. Golub, *Phys. Rev. B* 93 (2016) 045207.
- [3] L.E. Vorob'ev, E.L. Ivchenco, G.E. Pikus, I.I. Farbshtein, V.A. Shalygin, A.V. Shturbin, *JETP Lett.* 29 (1979) 441.
- [4] V.A. Shalygin, A.N. Sofronov, L.E. Vorob'ev, I.I. Farbshtein, *Phys. Solid State* 54 (2012) 2362.
- [5] R. Keller, W.B. Holzapfel, H. Schulz, *Phys. Rev. B* 16 (1977) 4404.
- [6] C. Hejny, M.I. McMahon, *Phys. Rev. B* 70 (2004) 184109.
- [7] L.A. Agapito, N. Kioussis, W.A. Goddard, N.P. Ong, *Phys. Rev. Lett.* 110 (2013) 176401.
- [8] M. Hirayama, R. Okugawa, S. Ishibashi, S. Murakami, T. Miyake, *JPS Conf. Proc.* 5 (2015) 011024.
- [9] M. Hirayama, R. Okugawa, S. Ishibashi, S. Murakami, T. Miyake, *Phys. Rev. Lett.* 114 (2015) 206401.
- [10] T. Hirahara, N. Fukui, T. Shirasawa, M. Yamada, M. Aitani, H. Miyazaki, M. Matsunami, S. Kimura, T. Takahashi, S. Hasegawa, K. Kobayashi, *Phys. Rev. Lett.* 109 (2012) 227401.
- [11] J. Ren, L. Fu, G. Bian, J. Su, H. Zhang, S. Velury, R. Yukawa, L. Zhang, T. Wang, G. Zha, R. Guo, T. Miller, M.Z. Hasan, T.-C. Chiang, *ACS Appl. Mater. Interfaces* 8 (2016) 726.
- [12] K. Hoefer, C. Becker, S. Wirth, L.H. Tjengb, *AIP Adv.* 5 (2015) 097139.
- [13] J. Park, Y.-A. Soh, G. Aepli, X. Feng, Y. Ou, K. He, Q.-K. Xue, *Sci. Rep.* 5 (2015) 11595.
- [14] G. Wang, X.-G. Zhu, Y.-Y. Sun, Y.-Y. Li, T. Zhang, J. Wen, X. Chen, K. He, L.-L. Wang, X.-C. Ma, J.-F. Jia, S.B. Zhang, Q.-K. Xue, *Adv. Mater.* 23 (2011) 2929.
- [15] T. Shirasawa, J. Tsunoda, T. Hirahara, T. Takahashi, *Phys. Rev. B* 87 (2013) 075449.
- [16] I. Kokubo, Y. Yoshiike, K. Nakatsuji, H. Hirayama, *Phys. Rev. B* 91 (2015) 075429.
- [17] T. Nagao, J. Sadowski, M. Saito, S. Yaginuma, Y. Fujikawa, T. Kogure, T. Ohno, Y. Hasegawa, S. Hasegawa, T. Sakurai, *Phys. Rev. Lett.* 93 (2004) 105501.